

A Novel Method for Efficient Numerical Stability Analysis of Delay-Differential Equations

Tamás Kalmár-Nagy

Abstract—It is shown that the method of steps for linear delay-differential equation can be formally used to find an infinite-dimensional linear map whose stability is equivalent to that of the delay equation. The truncated map can be used to estimate the spectrum of the discrete version of the evolution semigroup associated with the continuous equation. The method provides an efficient way to numerically determine stability regions in parameter space.

I. INTRODUCTION

There has been a recent surge of interest in numerical and analytical approximation of stability properties of linear delay-differential equations (DDEs). Transport delay is an inherent property of many physical and engineering systems. Stability analysis of DDEs is particularly important in control theory, where the delay is a consequence of finite-speed communication. A good exposition of delay equations as well as the study of their stability properties based on their characteristic equations can be found in [13]. Asl and Ulsoy [1] presented a new analytic approach to obtain the complete solution for systems of delay equations based on a Lambert-function expansion. The method of Olgac and Sipahi [12] is based on root counting and clustering to find stability regions. Breda et. al [3] presented an approach to compute the rightmost characteristic roots. Their method is based on the discretization of the infinitesimal generator of the solution operators semigroup and the approximation of the roots is obtained by a large sparse standard eigenvalue problem. Insperger and Stépán [8] extended the method of semidiscretization, which is common in structural dynamics to the study of DDEs. Semi-discretization utilizes the exact solution of linear systems over a short time interval to construct the mapping of a finite dimensional state vector for the system with time delay. Chen et al. [5] reformulated the characteristic equation as an equation in a single unknown and use a robust numerical technique for solving it. Butcher et al. [4] studied the stability properties of delay-differential equations with time-periodic parameters. By employing a shifted Chebyshev polynomial approximation in each time interval with length equal to the delay and parametric excitation period, the system is reduced to a set of linear difference equations for the Chebyshev expansion coefficients of the state vector in the previous and current

intervals. This defines a linear map which can be thought of as the ‘infinite-dimensional Floquet transition matrix’. Engelborghs and Roose [7] studied a numerical method to compute the characteristic roots based on multistep time-integration. Wahi and Chatterjee [16] used Galerkin-projection to reduce the infinite-dimensional dynamics of a DDE to one occurring on a finite number of modes. Shift operator induced approximations of delay systems were analyzed by Mäkilä and Partington [11] with the tools of robust control theory.

In the next Section, we re-introduce the age-old concept of the method of steps and in Section III. we show how this method can be used for stability analysis of a second-order delay-differential equation describing machine tool vibrations. Numerical results are presented in Section IV. and then Conclusions are drawn.

II. THE METHOD OF STEPS AND ITS USE FOR STABILITY ANALYSIS

Delay-differential equations may be solved as ordinary differential equations over successive intervals $[\sigma_k, \sigma_{k+1}]$ by the *method of steps* (see, for example [2]). The scalar DDE

$$x'(t) = f(t, x(t), x(t - \tau)) \quad t > 0 \quad (1)$$

with initial function $\Psi(t)$ defined on $t \in [-\tau, 0]$ is solved as a chain of differential equations

$$x'_1(t) = f(t, x_1(t), \Psi(t - \tau)) \quad 0 < t \leq \sigma_1 \quad (2)$$

$$x'_2(t) = f(t, x_2(t), x_1(t - \tau)) \quad \sigma_1 < t \leq \sigma_2 \quad (3)$$

$$\vdots \quad (4)$$

$$x'_m(t) = f(t, x_m(t), x_{m-1}(t - \tau)) \quad \sigma_{m-1} < t \leq \sigma_m \quad (5)$$

where $\sigma_l = l\tau$ for $l \in \mathbb{Z}^+$. Then $x(t) = x_l(t)$ for $t \in (\sigma_{l-1}, \sigma_l]$. While the method of steps has been extensively used in numerical solutions, it seems to have been overlooked as a potential candidate for linear stability analysis. For the purposes of stability analysis, the full knowledge of $x_l(t)$ on a given interval is unnecessary. The key idea of this paper is that stability of the $x(t) = 0$ steady-state solution can be determined from the behavior of the infinite sequence $\{x_l(\sigma_l)\}$ (which can be thought of as the τ -period Poincaré-map for the delay equation). Since on every $[\sigma_{l-1}, \sigma_l]$ interval we have a linear differential equation, the solution can be written down in closed form by using Laplace-transforms. The inverse Laplace-transform can then be used

This work was supported in part by the National Institute of Standards and Technology (NIST) ATP program, agreement number 70NANB4H3024

T. Kalmár-Nagy is with United Technologies Research Center, East Hartford, CT 06108, USA email:acc@kalmarnagy.com

to find where the initial conditions get mapped under the action of the equation. The spectrum of this discrete map reveals the stability properties of the original continuous system. This approximation corresponds to the discrete semigroup associated with the delay equation. Note that the method can readily be generalized to vector equations as well. Further, this idea can serve as a basis for stability analysis of equations with distinct, commensurate delays. Rigorous proofs will be presented in the sequel [10]. In the following we describe the implementation of this idea through an example.

III. IMPLEMENTATION

Consider the linear DDE

$$\ddot{x}(t) + 2\zeta\dot{x}(t) + (1+p)x(t) = px(t-\tau) \quad (6)$$

This differential equation describes linear stability of machine tool vibrations [9]. The stability curves (curves in (τ, p) -space where the characteristic polynomial of (6) has purely imaginary roots) can be expressed in closed form (parameterized by $\omega > 0$)

$$p = \frac{(1 - \omega^2)^2 + 4\zeta^2\omega^2}{2(\omega^2 - 1)} \quad (7)$$

$$\tau = \frac{2}{\omega} \left(j\pi - \arctan \frac{\omega^2 - 1}{2\zeta\omega} \right) \quad j = 1, 2, \dots \quad (8)$$

where $j > 0$ corresponds to the j th 'lobe' from the right in the stability diagram, and it can be shown that this system is stable for all parameter values below the lower bounding curve.

Taking the Laplace-transform of both sides of (6) results in

$$(s^2 + 2\zeta s + 1 + p)\mathcal{L}(x) - (s + 2\zeta)x_0 - v_0 = p\mathcal{L}(\psi) \quad (9)$$

where ψ is the initial function and x_0 and v_0 are the initial conditions for the state and its derivative at $t = 0$. For the first interval $(0, \tau]$ this equation can be solved for the Laplace-transform of $x(t)$ as

$$\mathcal{L}(x) = \frac{p\mathcal{L}(\psi) + g(s, x_0, v_0)}{h(s, p)} \quad (10)$$

with

$$g(s, x_0, v_0) = (s + 2\zeta)x_0 + v_0 \quad (11)$$

$$h(s, p) = s^2 + 2\zeta s + 1 + p \quad (12)$$

The states at the end of the interval can be calculated by calculating the inverse Laplace-transform of $\mathcal{L}(x)$ at $t = \tau$

$$x_1 = \mathcal{L}^{-1}(\mathcal{L}(x), \tau) = \mathcal{L}_\tau^{-1}(\mathcal{L}(x)) \quad (13)$$

$$v_1 = \mathcal{L}_\tau^{-1}(s\mathcal{L}(x)) \quad (14)$$

Now, since the states x_1, v_1 are known together with the 'new' initial function (or rather the Laplace transform of the new initial function), the equation can be solved on

$(\tau, 2\tau]$. The successive application of this procedure defines the following map

$$f_{n+1}(s) = \frac{pf_n(s) + g(s, x_n, v_n)}{h(s, p)}, \quad f_0(s) = \mathcal{L}(\psi) \quad (15)$$

$$x_{n+1} = \mathcal{L}^{-1}(f_{n+1}(s), \tau) = \mathcal{L}_\tau^{-1}(f_{n+1}(s)) \quad (16)$$

$$v_{n+1} = \mathcal{L}_\tau^{-1}(s f_{n+1}(s)) \quad (17)$$

A simple substitution of (16) into (15) results

$$x_{n+1} = \mathcal{L}_\tau^{-1} \left(\frac{pf_n(s) + g(s, x_n, v_n)}{h(s, p)} \right) = \quad (18)$$

$$\mathcal{L}_\tau^{-1} \left(\frac{g(s, x_n, v_n)}{h(s, p)} + \frac{pf_n(s)}{h(s, p)} \right) = \quad (19)$$

$$\mathcal{L}_\tau^{-1} \left(\frac{g(s, x_n, v_n)}{h(s, p)} + \frac{pg(s, x_{n-1}, v_{n-1})}{h^2(s, p)} + \frac{p^2 f_{n-1}(s)}{h^2(s, p)} \right) \quad (20)$$

Continuing the recursion, we arrive at

$$x_{n+1} = \mathcal{L}_\tau^{-1} \left(\sum_{i=0}^n \frac{p^i g(s, x_{n-i}, v_{n-i})}{h^{i+1}(s, p)} + \frac{p^n f_0(s)}{h^n(s, p)} \right) \quad (21)$$

Using the linearity of the inverse Laplace-transform

$$x_{n+1} = \sum_{i=0}^n p^i \mathcal{L}_\tau^{-1} \left(\frac{g(s, x_{n-i}, v_{n-i})}{h^{i+1}(s, p)} \right) + \\ p^n \mathcal{L}_\tau^{-1} \left(\frac{f_0(s)}{h^n(s, p)} \right) \quad (22)$$

Since linear stability should be independent on the choice of the initial function, we further assume that $f_0(s) = 0$. Thus

$$x_{n+1} = \sum_{i=0}^n p^i \mathcal{L}_\tau^{-1} \left(\frac{g(s, x_{n-i}, v_{n-i})}{h^{i+1}(s, p)} \right) \quad (23)$$

and similarly

$$v_{n+1} = \sum_{i=0}^n p^i \mathcal{L}_\tau^{-1} \left(\frac{sg(s, x_{n-i}, v_{n-i})}{h^{i+1}(s, p)} \right) \quad (24)$$

Since for any positive integer n the states (x_n, v_n) depend on all previous states, (23, 24) describe an infinite-dimensional system of difference equations. In matrix form

$$\begin{pmatrix} x_{n+1} \\ v_{n+1} \\ x_n \\ v_n \\ \vdots \end{pmatrix} = \underbrace{\begin{pmatrix} a_n & b_n & a_{n-1} & b_{n-1} & \dots \\ c_n & d_n & c_{n-1} & d_{n-1} & \dots \\ 1 & 0 & 0 & 0 & \dots \\ 0 & 1 & 0 & 0 & \dots \\ \dots & \dots & \ddots & \dots & \dots \end{pmatrix}}_{\mathcal{A}} \begin{pmatrix} x_n \\ v_n \\ x_{n-1} \\ v_{n-1} \\ \vdots \end{pmatrix} \quad (25)$$

It can be shown that the spectrum of the truncated system gets 'closer' to that of the infinite-dimensional system (25)

as the order is increased [10]. In our example

$$\begin{aligned} x_{n+1} = & \sum_{i=0}^n p^i \mathcal{L}_\tau^{-1} \left(\frac{s + 2\zeta}{h^{i+1}(s, p)} \right) x_{n-i} + \\ & \sum_{i=0}^n p^i \mathcal{L}_\tau^{-1} \left(\frac{1}{h^{i+1}(s, p)} \right) v_{n-i} \end{aligned} \quad (26)$$

$$\begin{aligned} v_{n+1} = & \sum_{i=0}^n p^i \mathcal{L}_\tau^{-1} \left(\frac{s(s + 2\zeta)}{h^{i+1}(s, p)} \right) x_{n-i} + \\ & \sum_{i=0}^n p^i \mathcal{L}_\tau^{-1} \left(\frac{s}{h^{i+1}(s, p)} \right) v_{n-i} \end{aligned} \quad (27)$$

and a_i, b_i, c_i, d_i can be read off from formulas (26, 27) as the coefficients of the corresponding x_i and v_i .

What remains is to numerically determine the coefficients a_i, b_i, c_i, d_i and to locate the spectrum of the matrix \mathcal{A} . Numerical inversion of Laplace-transforms has been an exponentially (pun intended) growing area since the seminal paper of Dubner and Abate [6]. The recent bibliography of Valkó and Vojta [15] lists several hundred papers in this area. It is also known (see for example [14]) that for a proper rational function $X(s)$ with real coefficients the inverse Laplace-transform can be expressed as a mixed exponential-power series

$$\mathcal{L}_\tau^{-1}(X(s)) = \sum_{i=1}^r \sum_{k=1}^{m_i} R_{ik} \frac{\tau^{k-1}}{(k-1)!} e^{p_i \tau} \quad (28)$$

where the p_i 's ($i = 1, \dots, r$) are distinct poles of $X(s)$ with multiplicities m_i . The residues R_{ik} can be computed from

$$R_{ik} = \frac{1}{(m_i - k)!} \lim_{s \rightarrow p_i} \frac{d^{m_i - k}}{ds^{m_i - k}} ((s - p_i)^{m_i} X(s)) \quad (29)$$

This formulation is well-suited to analytically study the properties of map \mathcal{A} .

IV. NUMERICAL RESULTS

Most commercially available numerical and symbolic software (such as MATLAB and Mathematica) have an efficient implementation of the inverse Laplace-transform. Here Mathematica was used to perform both the inverse Laplace-transforms and the eigenvalue calculations. For $\tau = 4.67, p = 0.1, \zeta = 0.01$ the first 6 coefficients are shown Table 1.

i	a_i	b_i	c_i	d_i
1	0.17	-0.89	0.98	0.18
2	-0.21	$-8 * 10^{-2}$	$-4 * 10^{-3}$	-0.21
3	$-9 * 10^{-3}$	$2 * 10^{-2}$	$-3 * 10^{-2}$	$-9 * 10^{-3}$
4	$1 * 10^{-3}$	$2 * 10^{-3}$	$-4 * 10^{-4}$	$1 * 10^{-3}$
5	$1 * 10^{-4}$	$8 * 10^{-5}$	$1 * 10^{-4}$	$1 * 10^{-4}$
6	$4 * 10^{-6}$	$2 * 10^{-6}$	$6 * 10^{-6}$	$4 * 10^{-6}$

Table 1. Coefficients of map (25)
for $\tau = 4.67, p = 0.1, \zeta = 0.01$

The coefficients very quickly (and monotonically in magnitude after the second terms) decay. The spectra for $\mathcal{A}_2, \mathcal{A}_5$, and \mathcal{A}_8 are shown in Fig. 1 together with the unit circle. Eigenvalues outside the unit circle represent unbounded solutions of the discrete map, thus imply the instability of the continuous system at the given parameter values.

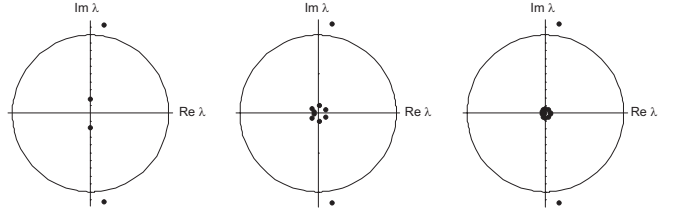


Fig. 1. Spectra for $\mathcal{A}_2, \mathcal{A}_5$, and \mathcal{A}_8 (left, middle, right). Parameter values $\tau = 4.67, p = 0.1, \zeta = 0.01$.

The spectra are also computed at the parameter values $\tau = 6.25135, p = 0.6481, \zeta = 0.01$. Here two of the stability lobes intersect, hence the resulting time response contains undamped oscillations at two distinct frequencies (the ratio of these frequencies is close to $3/2$). The spectra for $\mathcal{A}_2, \mathcal{A}_5, \mathcal{A}_{10}$, and \mathcal{A}_{15} are shown in Fig. 1. The

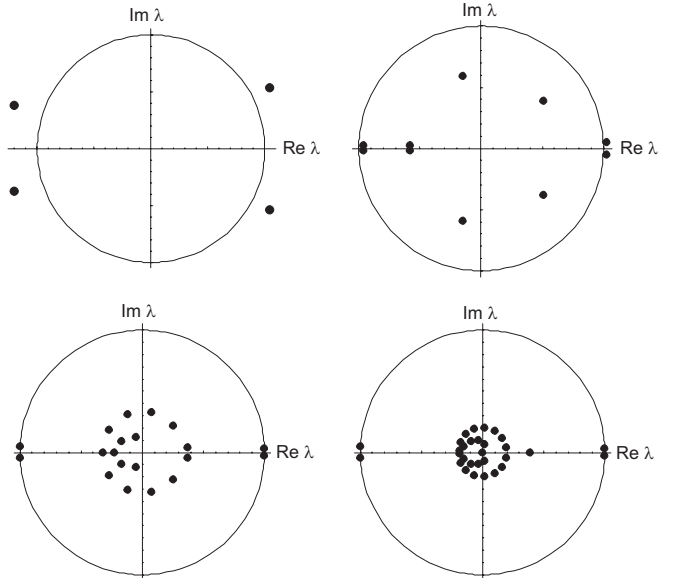


Fig. 2. Spectra for $\mathcal{A}_2, \mathcal{A}_5, \mathcal{A}_{10}$, and \mathcal{A}_{15} (top left, top right, bottom left, bottom right). Parameter values $\tau = 6.25135, p = 0.6481, \zeta = 0.01$.

two largest (in magnitude) pair of eigenvalues of \mathcal{A}_{15} are $0.9995 \pm 0.0309i$ and $-0.999 \pm 0.0467i$. These eigenvalues are very close to the unit circle, implying a superposition of a two-frequency undamped oscillation and other decaying modes for the continuous problem. Note that the ratio of the imaginary parts is close to $3/2$.

Finally, we use the method to numerically obtain a stability chart for (6). To determine stability of points on a grid in the (τ, p) space, we calculate the eigenvalues \mathcal{A}_5

corresponding to a fixed τ , p on the grid ($\zeta = 0.01$ is fixed). If all the eigenvalues are inside the unit circle, we deem system (6) stable at those parameter values, and color the gridpoint black. Fig. 3 shows the numerical stability chart together with the stability boundaries. Our method correctly

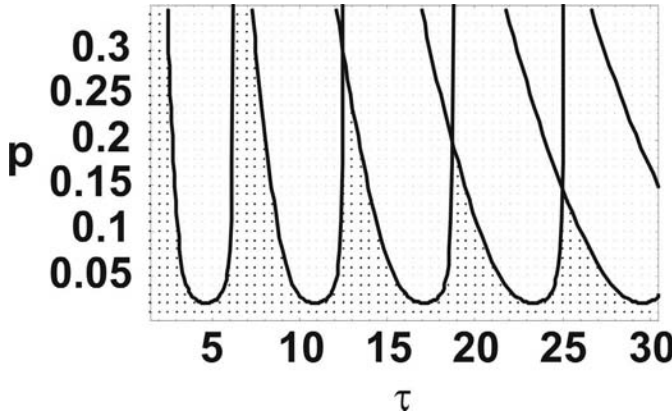


Fig. 3. Numerical stability chart for (6). Black points correspond to a stable system.

identifies the stable and unstable regions.

V. CONCLUSIONS

In this paper a new method utilizing the combination of the method of steps and numerical inversion of Laplace-transforms was introduced. At the heart of the method lies the truncation of the infinite-dimensional linear map, that acts on the initial values of the states at every time-delay interval. The method was shown to be simple, yet numerically effective in determining the stability of a delay-differential equation at a given point in parameter-space. While the convergence properties of the method are still under study, the efficiency and simplicity of the implementation is promising.

VI. REFERENCES

- [1] F. M. Asl and A. G. Ulsoy, Analysis of a System of Linear Delay Differential Equations, *Journal of Dynamic Systems, Measurement, and Control*, vol. 125, 2003, pp. 215-223.
- [2] C. T. H. Baker, C. A. H. Paul, and D. R. Wille, Issues in the numerical solution of evolutionary delay differential equations, *Advances in Comput. Math.*, vol. 3, 1995, pp. 171-196.
- [3] D. Breda, S. Maset, and R. Vermiglio, Computing the characteristic roots for delay differential equations, *IMA Journal of Numerical Analysis*, vol. 24, 2004, pp. 1-19.
- [4] E. A. Butcher, H. Ma, E. Bueler, V. Averina, and Zs. Szabó, Stability of time-periodic delay-differential equations via Chebyshev polynomials, *International Journal for Numerical Methods in Engineering*, vol. 59, 2004, pp. 895-922.
- [5] S.-G. Chen, A. G. Ulsoy, and Y. Koren, Computational stability analysis of chatter in turning, *Journal of Manufacturing Science and Engineering*, vol. 119, 1997, pp. 457-460.
- [6] H. Dubner and J. Abate, Numerical Inversion of Laplace Transforms by Relating Them to the Finite Fourier Cosine Transform, *Journal of the ACM (JACM)*, vol. 15(1), 1968, p.115-123.
- [7] K. Engelborghs and D. Roose, On stability of LMS methods and characteristic roots of delay differential equations. *SIAM J. Numer. Anal.*, vol. 40, 2002, pp. 629-650.
- [8] T. Insperger and G. Stépán, Semidiscretization method for general delayed systems, *International Journal for Numerical Methods in Engineering*, vol. 55, 2002, pp. 503-518.
- [9] T. Kalmár-Nagy, G. Stépán, and F. C. Moon, Subcritical Hopf bifurcation in the delay equation model for machine tool vibrations, *Nonlinear Dynamics*, vol. 26, 2001, pp. 121-142.
- [10] T. Kalmár-Nagy, A New Look at the Stability Analysis of Delay-Differential Equations, In preparation.
- [11] P. M. Mäkilä and J. R. Partington, Shift operator induced approximations of delay systems, *SIAM J. Control Optimiz.*, vol. 37, 1999, pp. 1897-1912.
- [12] N. Olgac and R. Sipahi, An Exact Method for the Stability Analysis of Time-Delayed LTI Systems, *IEEE Trans. Autom. Control*, vol. 47(5), 2002, pp. 793-797.
- [13] G. Stépán, *Retarded Dynamical Systems*. Longman: Harlow, UK, 1989.
- [14] D. V. Tošić and M. D. Lutovac, Symbolic computation of impulse, step and sine responses of linear time-invariant systems, *Symp. Theor. El. Engineering, ISTET*, Magdeburg, Germany, 1999, pp. 653-657.
- [15] P. P. Valkó and B. L. Vojta, The List, <http://pumpjack.tamu.edu/~valko>
- [16] P. Wahi and A. Chatterjee, Galerkin projections for delay differential equations, in *Proceedings of the ASME 2003 Design Engineering Technical Conferences*, Chicago, 2003, paper no. DETC2003/VIB-48574.